The Journal of Experimental Biology 216, 3395-3403

doi:10.1242/jeb.080317

RESEARCH ARTICLE

Hummingbird feather sounds are produced by aeroelastic flutter, not vortex-induced vibration

Christopher J. Clark[1,*], Damian O. Elias[2] and Richard O. Prum[1]

[1]Peabody Museum of Natural History, Yale University, PO Box 208106, New Haven, CT 06511, USA and [2]Department of Environmental Science, Policy and Management, University of California, Berkeley, 140 Mulford Hall, Berkeley, CA 94720, USA

*Author for correspondence at present address: Department of Biology, University of California, Riverside, CA 92521, USA (cclark@ucr.edu)

SUMMARY

Males in the 'bee' hummingbird clade produce distinctive, species-specific sounds with fluttering tail feathers during courtship displays. Flutter may be the result of vortex shedding or aeroelastic interactions. We investigated the underlying mechanics of flutter and sound production of a series of different feathers in a wind tunnel. All feathers tested were capable of fluttering at frequencies varying from 0.3 to 10 kHz. At low airspeeds (U_{air}) feather flutter was highly damped, but at a threshold airspeed (U^*) the feathers abruptly entered a limit-cycle vibration and produced sound. Loudness increased with airspeed in most but not all feathers. Reduced frequency of flutter varied by an order of magnitude, and declined with increasing U_{air} in all feathers. This, along with the presence of strong harmonics, multiple modes of flutter and several other non-linear effects indicates that flutter is not simply a vortex-induced vibration, and that the accompanying sounds are not vortex whistles. Flutter is instead aeroelastic, in which structural (inertial/elastic) properties of the feather interact variably with aerodynamic forces, producing diverse acoustic results.

Supplementary material available online at http://jeb.biologists.org/cgi/content/full/216/18/3395/DC1

Key words: aeroacoustic, sonation, tail, courtship display, wind tunnel.

Received 18 September 2012; Accepted 6 May 2013

INTRODUCTION

Birds produce non-vocal sounds during flight, especially during acrobatic displays (Bahr, 1907; Bahr and Pye, 1985; Bostwick and Prum, 2003; Bostwick and Prum, 2005; Clark et al., 2011a; Clark and Feo, 2008; Darwin, 1871; Hunter, 2008; Miller and Inouye, 1983; Prum, 1998). Flutter, in which airflow causes part of a feather to oscillate at audible frequencies, is the mechanism that produces tonal sounds during certain courtship displays of hummingbirds (Clark, 2008; Clark et al., 2011a; Clark and Feo, 2008) and snipe (Bahr, 1907; Carr-Lewty, 1943; Reddig, 1978). We tested a series of pennaceous (i.e. closed vaned) hummingbird feathers in a wind tunnel, and found that all feathers tested were capable of oscillating and producing tonal sound (Clark et al., 2011a). The sample included not only feathers that produce sounds in hummingbird courtship displays but also feathers that apparently do not produce sound during displays (Clark et al., 2011a). These data suggest that, as all wing and tail feathers are stiff and flat, all flight feathers may be susceptible to flutter.

Many other birds also produce tonal sounds during flight that are consistent with feather flutter (C.J.C. and R.O.P., manuscript in preparation), and production of non-vocal communication sounds appears to be evolutionarily labile (Prum, 1998). Understanding the mechanics of flutter will shed light on this potentially widespread mechanism of sound production in birds. In a previous study (Clark et al., 2011a) we did not explicitly consider the underlying mechanism. Here, we present further data on how hummingbird feathers flutter as a function of airspeed. We have split the analyses into two parts. In this paper, we explore the properties of flutter and ensuing sound as a function of airspeed that appear to be general across the feathers we tested. We also consider two alternative hypotheses of the origin of flutter, and present data rejecting one of these mechanisms, a vortex whistle mechanism. In the companion paper, we present tests of the structural resonance frequencies of the feathers we tested, and focus on how multiple types of modes of flutter and other types of non-linear behaviors add complexity to the underlying process we describe here (Clark et al., 2013).

As many, perhaps all, flight feathers can flutter when exposed to the right aerodynamic forces, we do not address which of the feathers tested here actually produces sound in wild birds. This topic was partially addressed in the supplemental online materials of our previous publication (Clark et al., 2011a), and will be more thoroughly addressed in future work. Likewise, we focus only on the sounds created by individual, isolated feathers in airflow as this is a relatively simple experimental paradigm, despite the demonstrated relevance of feather–feather interactions (such as amplification and heterodyne interactions) (Clark, 2011; Clark et al., 2011a). Finally, we take as a starting point the observation that the sounds we investigated here are tonal; we therefore ignore aperiodic (chaotic) flutter (Alben and Shelley, 2008; Manela and Howe, 2009b) as this does not produce tonal sound.

Fluid flowing around a solid structure, such as a feather, can result in dynamic oscillations in the solid and/or fluid (Bisplinghoff et al., 1996) that produces tonal sound. Self-sustaining periodic behavior is stable as a result of a feedback mechanism. A key mechanistic question is what roles the stiffness and resonance frequencies of the feather play in generating this feedback and ensuing sound. In the next two sections we develop two possible mechanisms.

One possible mechanism is a vortex whistle, in which the feedback mechanism is a consequence of intrinsically periodic fluid dynamic interactions with the geometry of the solid. Such aerodynamic mechanisms can be periodic when coherent vortices form and are shed by the object, generating a vortex street. Under this vortex whistle hypothesis, the elasticity and structural feedback of the solid are unimportant and stable oscillations and sound can be explained by the dynamics of vortex formation and shedding. Motion (flutter) is the result of fluid forcing alone, and the accompanying sound is referred to as a whistle (Chanaud, 1970). Alternatively, the feedback may lie in the exchange of fluid dynamic forces exerted on the solid, and the dynamic mechanical (elastic/inertial) forces of the solid exerted back on the fluid. In this case, the mechanism is aeroelastic (Bisplinghoff et al., 1996) and produces 'flutter-induced sound'. Our approach to testing these hypotheses was to test whether vortex formation in response to feather geometry alone is sufficient to explain the observed feather dynamics and sound production.

Vortex whistle hypothesis

Sound is generated when a flowing fluid interacts with a solid structure such as a feather (Blake, 1986). The relative motion of the feather shears the flow, causing it to acquire angular momentum, termed vorticity. Vorticity can be modeled as a spectrum of overlapping vorticies, where an element of this spectrum, a vortex, is an individual packet of rotating fluid with its own angular velocity and length scale (Blake, 1986). Any change in the strength of an individual vortex results in a change in pressure; therefore, as this vortex forms or dissipates, it produces sound (Blake, 1986; Lighthill, 1952). Vortex formation adjacent to a solid produces a dipole pattern of acoustic radiation (Blake, 1986). By contrast, a vortex dissipating well away from a solid boundary is a quadrupole sound source, which is a relatively inefficient acoustic radiator (Blake, 1986; Howe, 2008; Lighthill, 1952). For that reason, we neglect the sound produced by flow convecting away from the feather, and considered only the flow around the feather itself.

The formation of vorticity around a solid results in time-varying aerodynamic pressure (lift and drag), causing the solid to vibrate in forced response (Blake, 1986). At high Reynolds numbers, flow is turbulent and vortex formation is a broad-spectrum, random process, so the resulting vibration and sound is atonal, i.e. the familiar aerodynamic whooshing sounds of everyday life such as from an open window of a moving car. In flow regimes at Reynolds numbers that characterize the transition from laminar to turbulent flow (including much of bird flight), the fluid flow around an object can cause spatially coherent vortices to form and shed at a discrete frequency, such as a Von Kármán vortex street. Such vortex streets produce tones (Blake, 1986; Fletcher, 1992; Howe, 2008; Nash et al., 1999). In particular, vortex formation and shedding at frequency f causes cyclical fluctuations in the fluid forces on the object, with lift fluctuating at frequency f and drag at frequency $2f$ (Blake, 1986; Howe, 2008). Motion of the solid is in forced response to these forces (Bisplinghoff et al., 1996; Howe, 2008; Williamson and Gorvardhan, 2004) and it acts as a dipole radiator of sound. Because drag fluctuation has lower magnitude than lift (Blake, 1986; Howe, 2008), sound ensues primarily at f, with a weak 2nd harmonic at $2f$, and no higher harmonics. Other types of whistles may produce harmonics but these involve airflow interacting with a more complicated solid geometry, such as an 'edge whistle' caused by flow through an aperture and onto an edge (e.g. flute mouthpiece) (Blake, 1986; Chanaud, 1970; Fletcher, 1992; Howe, 2008), which we neglect here because a single feather lacks the necessary geometry.

This vortex whistle hypothesis predicts that vortex formation occurs at a constant Strouhal number (St):

$$St = fL / U_{\text{air}}, \quad (1)$$

where U_{air} is air flow velocity and L is an appropriate length scale, such as the thickness of the boundary layer [e.g. table 11.3 in Blake (Blake, 1986)]. Though the classic examples of vortex whistles are non-streamlined bodies such as a 'singing' telephone wire, streamlined airfoils can also whistle by this mechanism (Blake, 1986; Nash et al., 1999). Moreover, the relationship $f \propto U_{\text{air}}$ of Eqn 1 is also found in models of flutter that disregard airfoil stiffness, such as eqn 20 of Argentina and Mahadevan (Argentina and Mahadevan, 2005). Similarly, Manela and Howe (Manela and Howe, 2009a; Manela and Howe, 2009b) modeled the motion of an unforced flag. In the limit of negligible stiffness, flutter may be chaotic (see also Alben and Shelley, 2008) unless periodicity is regulated by a fluid-generated process, such as upstream vortex formation (Manela and Howe, 2009a; Manela and Howe, 2009b).

This vortex whistle model makes two predictions. Sound frequency is predicted to scale linearly with flow velocity (Eqn 1), and harmonics above $2f$ are not expected. Under this whistle model, any motion of the feather is a forced response to the fluid flow, i.e. the motion is a vortex-induced vibration (Williamson and Gorvardhan, 2004).

Aeroelastic flutter hypothesis

Alternatively, sound is generated by an aeroelastic process, i.e. the stiffness and accompanying resonance frequencies of the airfoil are not negligible and play an important role in the dynamics of oscillation (Bisplinghoff et al., 1996). Airflow across the feather provides aerodynamic energy, which may or may not be in the form of discrete vortices. This excites one or more structural resonance frequencies within the feather, creating stable oscillations (Bisplinghoff et al., 1996; Mandre and Mahadevan, 2010; Manela and Howe, 2009b). Aeroelastic flutter is hypothesized to exhibit a critical velocity, U^*, below which the feather's damping exceeds the energy received from airflow, and flutter does not occur (Argentina and Mahadevan, 2005; Bisplinghoff et al., 1996; Mandre and Mahadevan, 2010). At U^*, damping is overcome, and oscillations increase in amplitude as a result of positive feedback between aerodynamic and structural (inertial and elastic) forces.

This hypothesis does not invoke the existence of spatially discrete vortices that form around the feather and drive its motion. However, it does not categorically rule out their presence either; rather, it proposes that the observed dynamics are not predicted or explained by vortex formation and shedding. As in other objects that vibrate *via* structural resonance and have continuous energy input, such as a violin string, non-linearities are expected. For example, multiple resonance frequencies may be stimulated simultaneously, in which case harmonics may become mode-locked to the fundamental frequency, resulting in acoustic harmonics that are integer multiples of the fundamental (Fletcher and Rossing, 1998). If mode-locking does not occur, feathers could also exhibit simultaneous unrelated modes of vibration. The difference between the aeroelastic flutter hypothesis and the whistle hypothesis is the importance of feather mass and stiffness, which add complexity to a feather's acoustic behavior at U_{air} above U^*.

MATERIALS AND METHODS

Feathers

Hummingbirds in the 'bee' clade (McGuire et al., 2009) have tail feathers (rectrices) that vary in size, shape and stiffness (Clark, 2011;

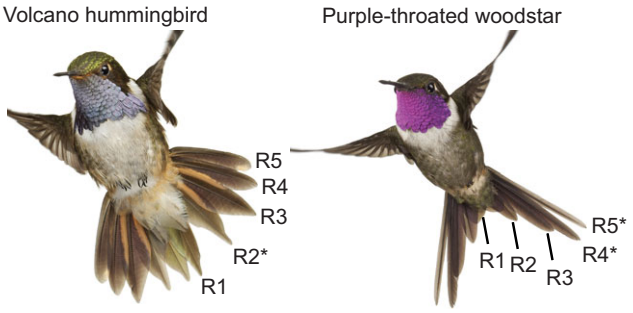

Fig. 1. Two male hummingbirds with inner (R1) to outer (R5) rectrices labeled. Astrisk indicates feathers tested in this study. Photos courtesy of Anand Varma. Image of volcano hummingbird re-used (from Clare et al., 2011b) with permission from *The Wilson Journal of Ornithology*.

Clark et al., 2011a; Clark and Feo, 2008; Clark and Feo, 2010; Clark et al., 2011b). Hummingbirds have five pairs of rectrices, which are numbered R1 to R5 (Fig. 1). We tested a series of rectrices from males of 14 bee hummingbird species, which are listed in supplementary material Table S1. Feathers used in this study were obtained from wild birds under the relevant collecting and import permits.

Geometric framework

A pennaceous feather has a central shaft, the rachis. Projecting out from either side of the rachis are barbs with differentiated distal and proximal barbules that interlock to form a flat, planar surface, the vane (Fig. 2). These barbules can temporarily become unzipped from one another, causing gaps to appear in the vane; birds fastidiously preen their feathers to maintain an intact vane with barbs fully interlocked. At the feather's base, the rachis inserts into the feather follicle *via* a straight, barbless region called the calamus.

We mounted the feathers by the calamus so that they projected down into the working section of a wind tunnel (below). A feather's *X*-axis was parallel to airflow, the *Y*-axis was vertical, and the *Z*-axis was perpendicular to *X* and *Y* (Fig. 2A). The wind tunnel flow regime was non-accelerating freestream flow (U_{air}). Rotation about the *Y*-axis changed the angle of attack (α), while rotation about the *Z*-axis changed the sweep angle (β), both of which affected the aerodynamic forces upon the feather. By contrast, rotation about *X* was irrelevant as this axis was parallel to flow and so rotations about *X* do not change the magnitude of aerodynamic forces on the feather. We centered the origin at the calamus (Fig. 2A). We did not quantify α or β, because variable aeroelastic deformation (bending and twisting) meant these variables were not defined down the length of the feather, making quantitative comparisons as a function of α or β difficult to interpret.

The relevant independent variables influencing a feather's responses to airflow were orientation (α and β), size, stiffness, shape and aeroelastic deformation. Aeroelastic deformation, for our purposes, specifically refers to the significant static bending

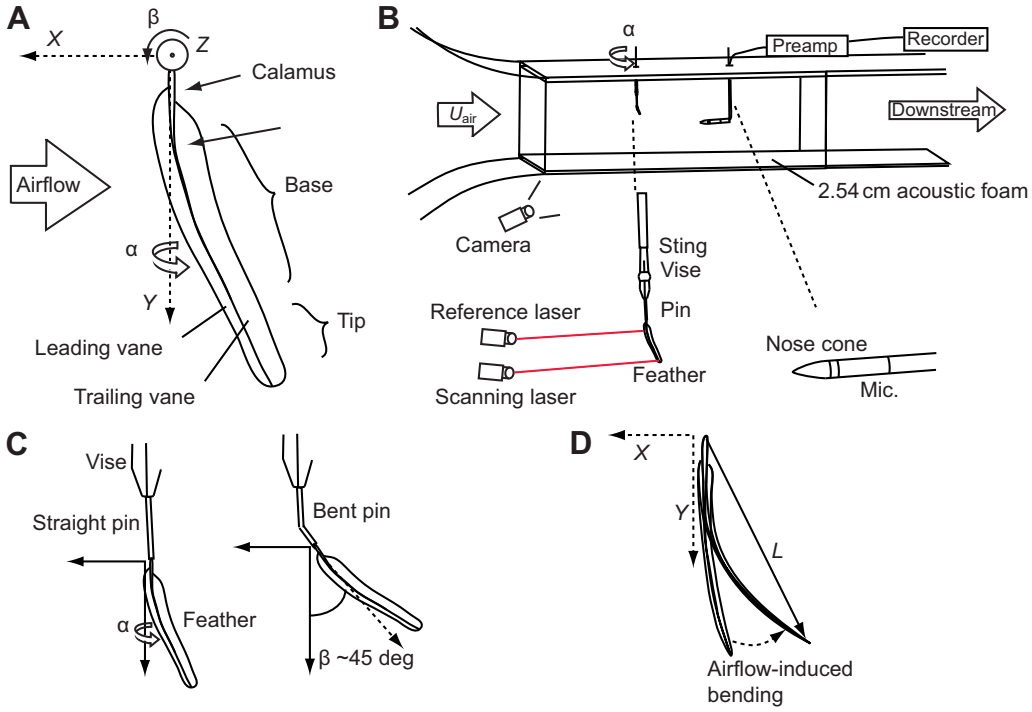

Fig. 2. Experimental setup and coordinate system. (A) Lab-based coordinate system (side view). Rotation about *Y* was angle α and rotations about the *Z*-axis (projects out of the page) was angle β. These angles were defined at the feather's calamus, where aeroelastic deformation was negligible. Feather is R5 from Anna's hummingbird. (B) Experimental setup used to record sounds, vibrations and video of feathers in the working section of a wind tunnel. A sting projected into the working section from the top of the wind tunnel, and could be rotated about its longitudinal axis from outside the tunnel (rounded arrow). The feather was glued to a pin, which was mounted in a pin vise attached to the end of the sting. The microphone was not in the aerodynamic wake of the feather. The top and bottom surfaces of the tunnel were lined with 2.54 cm acoustic foam. The lasers (described in Clark et al., 2013) and camera recorded the feather through the acrylic walls of the tunnel. (C) The sting could be rotated from outside the wind tunnel, changing α, whereas β was changed by bending the pin to which the feather was glued. (D) Under this coordinate system, angles α and β did not shift when feathers bent or twisted in airflow; these are changes in aeroelastic deformation. As a result, this feather's orientation did not change, even though airflow-induced bending may result in a large shift in the feather's longitudinal axis (*L*). R4 from white-bellied woodstar.

and twisting all feathers experienced in response to imposed aerodynamic forces, independent of any oscillatory behavior of flutter itself. This is distinct from a feather's 'shape', which specifically refers to feather geometry in the absence of flow, with all barbs fully interlocked. Airflow-induced aeroelastic deformation did not constitute a change in orientation (e.g. Fig. 2D) because of how we defined the coordinate system. Therefore, a feather's geometry as a function of airflow was not well specified: at each U_{air}×α×β combination, every feather exhibited unique aeroelastic deformation that we lacked the means to quantify. Because flutter is also an aeroelastic phenomenon, it was not possible to clamp multiple parts of the feather to control aeroelastic deformation.

The dependent variables investigated were: mode of flutter, flutter frequency, flutter velocity (i.e. amplitude), sound frequency and loudness. We quantitatively investigated the effects of U_{air} on all of these dependent variables, and qualitatively investigated the influence of α, β, shape, stiffness and aeroelastic deformation.

Wind tunnel

The acoustic properties of individual feathers were tested in the working section of an Eiffel-style open wind tunnel in the Department of Mechanical Engineering at Yale University, near sea level. The usable area of the working section measured 61 cm wide by 33 cm tall, with a contraction area ratio of 8.75. Feathers were mounted ~10 cm below the ceiling. Air was drawn through the working section with a centrifugal fan. U_{air} could be continuously varied from 0 to >40 m s^{-1}. After the tunnel was acoustically prepared for this experiment (see below), velocity was calibrated using a Pitot tube attached to a pressure transducer.

The wind tunnel was not designed for acoustic experiments, and had relatively high noise within the test section. The motor produced substantial background sound even at low speeds. Airflow created vortex whistles around permanent fixtures within the working section, which we individually eliminated or ignored. To further reduce background noise and reverberation, 2.54 cm acoustic foam (noise reduction coefficient: 0.72) was mounted on the floor and ceiling of the tunnel (Fig. 2B). The acoustic treatment reduced background levels of sound at octave bands above 1 kHz by 11.4 dB at 20 m s^{-1}, but had limited effects on background noise below 1 kHz, which was also the frequency band with the most noise. Spectrograms from the working section before and after acoustic treatment are presented in supplementary material Fig. S1. Background aerodynamic noise increased with U_{air} (supplementary material Fig. S1).

Sound was recorded with a 0.5 in free-field microphone (Brüel & Kjaer 4190, Naerum, Denmark) with a turbulence-reducing nose cone (B&K UA 0386), suspended in the free-stream of the wind tunnel, ~10 cm downstream from (but not in the wake of) the test subject (Fig. 2B). The microphone was less than 1 wavelength of the source for sounds <3.3 kHz. The microphone and nose cone had a flat frequency–response curve (±3 dB) between 3 Hz and 15 kHz (Soderman and Allen, 2002). Output from the microphone was routed through an amplifier to a 24 bit recorder that sampled at 48 kHz (Sound Devices 702, Reedsburg, WI, USA). The microphone was calibrated with a B&K 4231 sound level calibrator. Based on the microphone's distance from the feather, sound pressure levels (SPL; re. 20 μPa) at 1 m from the source were calculated assuming a uniform (monopole) pattern of sound radiation, and assuming that near-field effects were negligible. Both of these assumptions were violated, but this bias was likely constant across recordings for an individual feather (see Discussion). Minimum reflection distance from the non-acoustically treated surfaces of the tunnel was ~0.6 m, therefore reverberation was ignored. Sounds were analyzed in Raven 1.3 (www.birds.cornell.edu/raven) and presented as spectrograms and waveforms. Because the sounds were invariant over time, spectrograms were generated with a window size of >10,000 samples to maximize frequency resolution.

To mount the feathers, an insect pin was inserted into the calamus, with a small amount of cyanoacrylate glue. The head of the pin was removed, and the portion of the pin projecting from the feather was inserted into a pin vise at the end of a sting that projected down from the top of the tunnel (Fig. 2B,C). With the airflow turned on, the feather could be rotated around the *Y*-axis (angle α) from the outside of the tunnel (Fig. 2A). In order to change β, the pin connecting the feather to the pin vise was bent, with the airflow off (Fig. 2C).

High speed video of a subset of the feathers in the wind tunnel was obtained with a Phantom Miro EX4 (Vision Research, Wayne, NJ, USA) filming at 23,121 frames s^{-1}. The feather was backlit with an incandescent light.

Wind tunnel experiments

Our goal was to study the onset of flutter as a function of feather size, shape and U_{air}, at a constant orientation. We did not quantitatively explore the relationship between orientation (α and β) and other relevant parameters (such as U_{air}) for several reasons. First, as described above, feather aeroelastic deformation varied greatly, making comparisons between feathers as a function of α and β ambiguous. Second, our experimental setup only allowed us to vary α precisely with the airflow on (Fig. 2), while adjustment of β was crude, impairing our ability to explore all pair-wise combinations of α and β. Third, the range of angles over which a feather vibrated in a particular mode was sometimes relatively narrow, and in extreme cases, rotating a feather as little as 2 deg in either direction would cause jumps in vibratory behavior (see Clark et al., 2013). Therefore, very small steps in angle would be necessary to quantitatively map a feather's behavior as a function of α and β, and result in an unfeasibly large number of samples necessary. We quantitatively examined the onset and behavior of flutter as a function of feather size, shape and U_{air} at a single, constant orientation, while we qualitatively explored the relationship between orientation and other variables.

We selected a test orientation by placing the feather in the tunnel in an orientation simulating that feather in a flying bird with its tail widely spread (Fig. 1). Outer rectrices (R4 or R5) were mounted with an un-bent pin (β ~0 deg) such that rotating the sting caused changes in α. Inner tail feathers (R1, R2 or R3) had the attachment pin bent up to β=45 deg so that rotating the sting caused the feather to move through a combination of α and β. The tunnel was set to a relatively high speed, ~20 m s^{-1}, for most feathers. The sting was then rotated through a range of angles (typically −90 to 90 deg) until the feather fluttered and produced sound. In many cases, we immediately found a mode of flutter that matched the dive-sound of the bird it was from. If we did not, we stopped the tunnel and bent the pin to a new value of β so that rotating the sting would explore a new range of orientations. The feather was tested at up to five pin orientations at up to three relatively high values of U_{air}. If a mode of vibration was not found that matched that made by the bird (as expected if the feather being tested does not make the sound produced by the bird), we tested the feather in an orientation in which it expressed the loudest, most consistent mode of flutter.

Once a feather's orientation was set, U_{air} of the tunnel was first decreased in increments of ~0.75 m s^{-1}. After a speed had been

reached in which the feather no longer vibrated or produced sound, U_{air} was returned to the starting speed, and then increased in increments of 0.75 m s^{-1}. We measured feather vibration amplitude directly using a SLDV (PSV-I-400 LR, OFV-505 scan head fitted with a close-up attachment PSV-A-410, Polytec Inc., Irvine, CA, USA). For details, see the accompanying paper (Clark et al., 2013).

RESULTS

All feathers tested in the wind tunnel were capable of fluttering and producing audible tones. SLDV measurements revealed a nearly 1:1 correspondence between flutter and sound recorded by the microphone (Clark et al., 2011a). Consistent with the aeroelastic flutter hypothesis, all modes of flutter exhibited a critical velocity, U^*, below which flutter amplitude was minute and no sound was produced, and above which flutter amplitude was high and sound was produced (Fig. 3). No tonal sounds were associated with the feathers in the absence of feather motion.

Fig. 3 shows three examples of three ranges of vibratory behavior (I, II and III) in airflow. An expanded version of Fig. 3 showing the corresponding vibratory and acoustic spectra is presented in the supplementary material Fig. S2. These three ranges of vibratory behavior were exhibited by all feathers tested. At low U_{air}, which we term range I, the feathers were immobile, and velocity power spectra from the SLDV revealed no peaks that exceeded an average velocity of 0.0001 m s^{-1} (supplementary material Fig. S2C,E,G). As U_{air} increased, low-amplitude motion at discrete frequencies in the feathers was detected by SLDV, which we termed range II. At a critical velocity (U^*), the amplitude of the motion abruptly increased as the feather entered range III and, simultaneously, sound was detected above the background of the wind tunnel (supplementary material Fig. S2: compare B with C, D with E, and F with G). Above U^*, all of the feathers had individual points that reached speeds exceeding the 3 m s^{-1} limit of the SLDV, so all of our measures of average velocity within range III are underestimates (Clark et al., 2013). We hypothesize that average flutter amplitude increased or remained constant with U_{air} in range III of all feathers, and that data suggesting otherwise (e.g. red squares in range III of Fig. 3; supplementary material Fig. S2A) are an artifact resulting from the measurement limits from the SLDV.

The range of U_{air} at which a feather fluttered and produced sound was bounded; each mode of flutter appeared to have its own critical velocity, which set the lower speed at which it will produce sound. Multiple mechanisms appear to set the upper speed. Most commonly, at high U_{air} the barbs on the feather started to become unzipped. This changes the shape of the feather, and either flutter ceased completely or loudness decreased. In a few cases, feathers ceased stable oscillations and instead fluttered chaotically. Finally, in some cases, at high test speeds the rachis or calamus of the feather suddenly broke. Such failure seemed to be caused or facilitated by flutter (see Clark et al., 2013).

Most of the feathers exhibited a positive correlation between loudness and U_{air} (Fig. 4A) across the range of U_{air} tested. Five did not: rufous hummingbird (*Selasphorus rufus*) R2, scintillant hummingbird (*Selasphorus scintilla*) R2, broad-tailed (*Selasphorus platycercus*) R2, purple-throated woodstar (*Philodice mitchellii*) R4 and magenta-throated woodstar (*Philodice bryantae*) R5 (Fig. 4A). Average feather velocity was also correlated with loudness in most but not all feathers (Fig. 4B). Our estimates of 'average velocity' were biased as a result of limits on the SLDV (Clark et al., 2013). The feathers with negative slopes in Fig. 4B tended to exhibit tip modes of vibration for which this artifact was especially strong. We

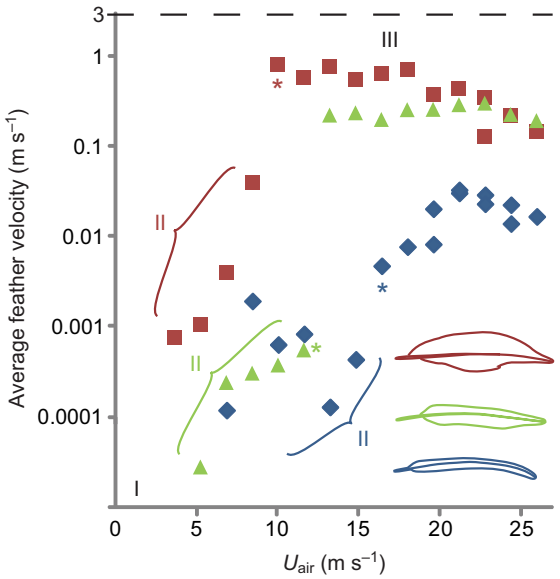

Fig. 3. Sound production and average flutter velocity as a function of airspeed (U_{air}), for Costa's hummingbird (*Calypte costae*) R5 (blue), volcano hummingbird (*Selasphorus flammula*) R2 (red) and black-chinned hummingbird (*Archilochus alexandri*) R5 (green). All feathers exhibited varying magnitudes of flutter that fitted into three ranges. Range I: at low U_{air}, no motion was detected (no data present). Range II: at intermediate U_{air}, small amplitude vibrations were recorded, but no sound was detected (braces). Asterisk indicates the sound first detected. The transition from range II to range III occurs at a critical velocity (U^*) characterized by an abrupt increase in vibration velocity. The scanning laser Doppler vibrometer (SLDV) had a maximum velocity of 3 m s^{-1} (dashed line) that results in a downward bias of the points in range III, as the graphed points represent averages of all points across the feather that could be scanned. An extended version of this figure is presented in supplementary material Fig. S2, which shows sound spectrograms and SLDV vibration spectra corresponding to the data plotted here; plotted points reflect the peak velocity of the fundamental frequency of vibration.

suggest that the negative slopes in Fig. 4B are not real, but are entirely attributable to this limitation to the SLDV measurements.

Fundamental frequency of vibration was positively correlated with U_{air} in most of the feathers (Fig. 5), and all feathers exhibited ranges of speeds over which the frequency–velocity relationship was linear (i.e. incremental changes in air velocity resulted in incremental changes in frequency). However, changes in U_{air} sometimes caused obvious mode jumps, in which the mode shape of flutter abruptly and dramatically shifted from one mode to another, such as from a tip mode to a trailing vane mode (see Clark et al., 2013). These were accompanied by an abrupt change in frequency. Large, between-type mode jumps (which could be easily, unambiguously diagnosed) have been omitted from Fig. 5; examples of hypothesized within-type mode jumps (which could not be unambiguously diagnosed) are indicated with arrows (Fig. 5A). Note that for purposes of comparison, Fig. 5 depicts only the fundamental frequency of flutter, not the integer harmonics, despite the fact that the integer harmonics were usually prominent and sometimes contained more energy than the fundamental.

The patterns of feather behavior in the wind tunnel were inconsistent with the vortex whistle hypothesis. Under this hypothesis, vortex shedding was predicted to occur at a constant St. As we do not have an estimate of L appropriate for calculating St, we substituted the reduced frequency (fL/U_{air}) for St, deriving length

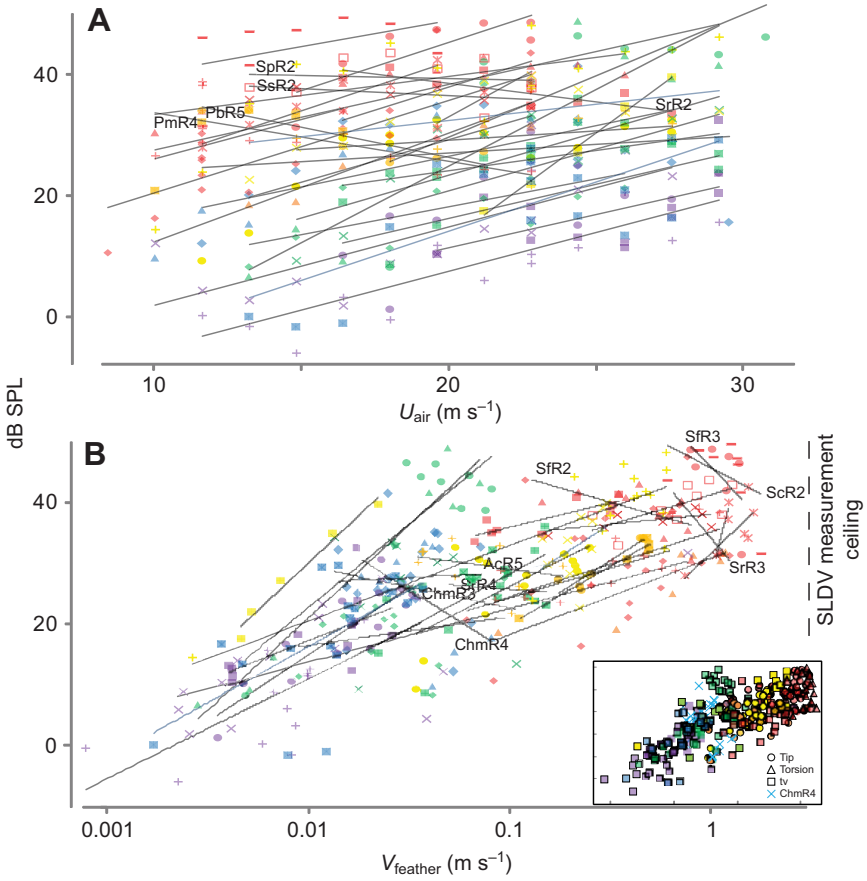

Fig. 4. Loudness as a function of feather velocity ($V_{feather}$, averaged across all sampled points on the feather), airspeed (U_{air}) and frequency, for 31 hummingbird tail feathers. (A) Loudness plotted against airspeed. (B) Loudness plotted against average velocity of points measured across a feather. Lines are regressions for individual feathers. Color encodes average frequency (in kHz): red <0.95, orange 0.96–1.55, yellow 1.56–2.41, green 2.42–4.8, blue 4.9–7.2, purple >7.3. Feathers with negative slopes are labeled; the first two/three letters indicate species and the second two are feather (R1 to R5): Pm, *Philodice mitchellii*; Pb, *Philodice bryantae*; Chm, *Chaetocercus mulsant*; Ss, *Selasphorus scintilla*; Sp, *Selasphorus platycercus*; Sr, *Selasphorus rufus*; Sf, *Selasphorus flammula*; Ac, *Archilochus colubris*. The SLDV could only measure up to 3 m s^{-1}, biasing the averages depicted here. See the companion paper (Clark et al., 2013) for further details. Inset in B shows the same data replotted with different shapes indicating the mode of flutter; tv, trailing vane.

L from feather width; this dimension was not parallel to flow in all feathers, particularly those with 'tip' modes. Reduced frequency varied by an order of magnitude among the feathers tested, and in all feathers significantly declined with increasing airspeed (Fig. 5B). The ability of *Chaetocercus mulsant* R4 to vary pitch continuously by 40% at a constant U_{air} is not explained by the vortex shedding hypothesis [see fig. 2 in the companion paper (Clark et al., 2013)]. Essentially, all feathers produced loud higher harmonics, and some feathers had 30 or more harmonics (supplementary material Fig. S2D). Moreover, individual feathers exhibited several types of non-linear responses to airflow not predicted by the vortex whistle hypothesis. Abrupt changes in mode of flutter were present in nearly all feathers (arrows in Fig. 5A). Additional types of non-linearities were occasionally present (see Clark et al., 2013), and included multiple (non-mode locked) modes of flutter expressed simultaneously, harmonic dominance (including loss of all odd harmonics, i.e. period-halving) and the presence of partials (non-integer harmonics). Harmonic content of the sound varies with how the feather is aerodynamically activated, much as the harmonics of a violin depend on how it is bowed (Fletcher and Rossing, 1998).

DISCUSSION

In this study, we examined the aeroacoustic behavior of hummingbird tail feathers that vary in shape over a range of air velocities in a wind tunnel. All feathers tested fluttered and produced sound in the wind tunnel and many, though not all, of these feathers appear to have evolved acoustic functionality in courtship displays of these birds [see online appendix of our previous publication (Clark et al., 2011a)]. The predictions of the vortex whistle hypothesis were not supported. Thus, vortex formation and shedding are not sufficient to explain sound production by these feathers. In the companion paper (Clark et al., 2013) we show that the onset of flutter coincides with discrete structural resonance frequencies of feathers, providing further support for the aeroelastic flutter hypothesis. We conclude that hummingbird feathers do not whistle: flutter of the hummingbird feathers is aeroelastic, the result of a complex feedback between airflow, and geometric and material properties of the feather.

The feathers tested here differed primarily in shape (Fig. 5) and did not vary much in size (dimensions in supplementary material Table S1; vane thickness is on the order of 10 μm). As all feathers are made of β-keratin (Bonser and Purslow, 1995; Brush, 1983), the feathers tested here were of similar elastic modulus. Therefore, we suggest the same mechanism applies to all of the feathers, and attribute the measured differences between the feathers to these small differences in size and shape.

In contrast with our conclusion, van Casteren and colleagues (van Casteren et al., 2010) attribute the sounds produced by common snipe (*Gallinago gallinago*) outer tail feathers to vortex shedding. However, inconsistencies and omissions undercut this conclusion. They claim that individual snipe rectrices tested in a wind tunnel did not produce harmonics. However, Reddig (Reddig, 1978) did produce strong harmonics from snipe rectrices in this manner, contra to the whistle hypothesis. Reddig's (Reddig, 1978) result is accurate, as the sounds he elicited match the sound of actual snipe performing their 'winnowing' or 'drumming' displays, which include over a dozen prominent harmonics [see fig. 3 in Reddig (Reddig, 1978), or recordings of display sounds on www.xeno-canto.org]. One cause of the discrepancy may be the fast Fourier transform (FFT) window size of 1024 samples that van Casteren and colleagues (van Casteren et al., 2010) used to analyze their data. This window size is appropriate for time-varying data such as bird song, but has relatively poor frequency resolution. This may obscure harmonics

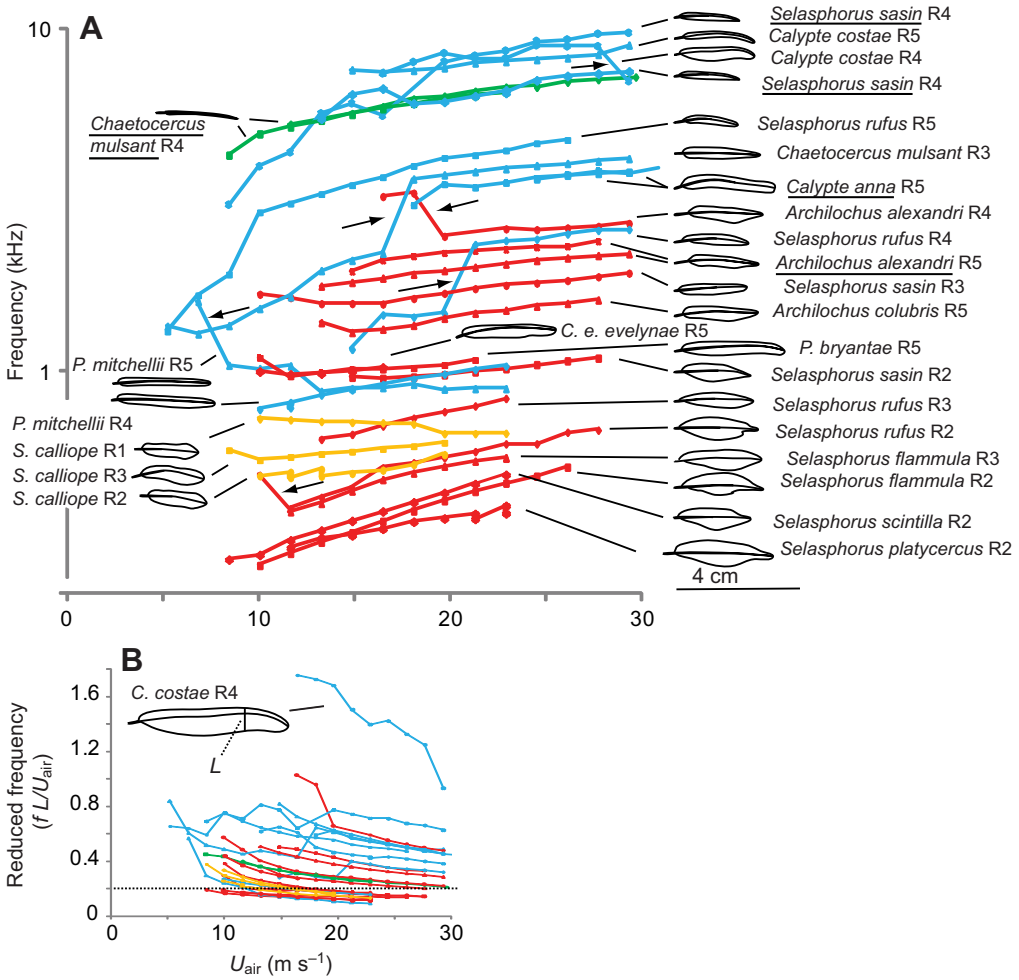

Fig. 5. (A) Fundamental frequency of vibration (from SLDV data) and (B) reduced fundamental frequency as a function of U_{air}, for 30 feathers of 26 types [replotted from Clark et al. (Clark et al., 2011a)]. Color indicates the type of mode exhibited by the feather: blue, trailing vane; red, tip; yellow, torsional; and green, white-bellied woodstar (*Chaetocercus mulsant*) R4. Mode jumps that switch between types of modes (e.g. from a tip mode to a trailing vane mode) have been omitted; see the companion paper (Clark et al., 2013) for a description of this phenomenon. Abrupt changes in frequency are indicated with arrows. We hypothesize that these represent mode jumps within a mode type (e.g. a jump from one type of tip mode to another), but this could not be unambiguously diagnosed from our data. Feather outlines are traced from photos. The abbreviated species names are *Philodice mitchellii*, *Selasphorus calliope*, *Philodice bryantae* and *Calothorax e. evelynae*. Note the logarithmic *y*-axis. N=1 for all feather types except those underlined, for which N=2 samples (there is almost complete overlap for the replicate *Chaetocercus mulsant* R4 and *Calypte anna* R5 samples). (B) Reduced frequency of flutter as a function of U_{air}. Length L is indicated; this length was approximately parallel to flow for feathers exhibiting trailing vane modes (blue), whereas it was at an oblique angle to flow for the remaining feathers. The horizontal dotted line indicates the reduced frequency predicted by vortex shedding. Reduced frequency declined with airspeed for all feathers.

in a recording taken in a noisy environment such as a wind tunnel. As the sound recorded in a wind tunnel is time-invariant, a larger FFT window was warranted. van Casteren and colleagues (van Casteren et al., 2010) also found that snipe feathers flutter at half the vortex-shedding frequency they had predicted, but explain the twofold difference by suggesting that two vortices were shed per vibratory cycle. This misunderstands the convention for the Strouhal number: for every one cycle of vortex shedding, two vorticies of opposite sign are shed, so the vortex-shedding frequency should match the flutter frequency (Bearman, 1984; Rayleigh, 1915; Williamson and Gorvardhan, 2004). In conclusion, the sounds generated by snipe feathers do not appear to be the result of vortex shedding.

The vortex whistle hypothesis does not make predictions that are supported by the available data, suggesting that vortex formation does not drive flutter. This conclusion does not imply a lack of vorticity or vortical structures in the air around a fluttering feather. Clearly, vorticity must form and be shed by the feather, because of the presence of sheared flow. Our data suggest several predictions about the vorticity of a fluttering feather. Given the (usually) coherent nature of both the feather's kinematics and the recorded sound, the vorticity probably forms coherent vortical structures. The feather's kinematics were sometimes spatially complex, with different regions moving with differing frequencies and/or phase. This suggests a similar spatial complexity to any vortical structures. Likewise, the sounds and feather motions we recorded constituted a harmonic series (supplementary material Fig. S2) (Clark et al., 2011a) and as the feathers tested here are compact sound sources (physical dimensions < sound wavelength), any such vortical structures will have a corresponding harmonic component. This complexity is likely to be greatest in feathers exhibiting tip modes of vibration (Clark et al., 2013), as well as snipe feathers (Reddig,

1978), as these tended to have dozens of harmonics (e.g. supplementary material Fig. S2) (Reddig, 1978). These predictions do not prescribe some sort of '1 motion–1 vortex' model. For fluttering filaments and actuated airfoils, it has been clearly shown that there need not be a 1:1 relationship between shed vortices and the structure's oscillatory motion (Lentink et al., 2010; Schnipper et al., 2009; Zhang et al., 2000; and references therein).

We suggest that aerodynamic excitation of a feather causes it to flutter when aerodynamic energy received exceeds structural damping, and that periodicity is set in part by the structural resonance of the feather. Our wind tunnel data on hummingbird flight feathers support this aeroelastic flutter hypothesis. All feathers that we measured exhibited distinct behavior over three ranges of airspeeds (Fig. 3; supplementary material Fig. S2). In range I (low U_{air}), the SLDV detected no feather motion above the noise floor of the device. In range II, low amplitude motions of the feathers were measured, and the peak frequencies and feather regions most activated by flow tended to shift or move somewhat unpredictably with small changes in speed (e.g. supplementary material Fig. S2C). These motions were not visible, and appeared to be highly damped. The transition from range II to range III (i.e. U^*) was typically sudden; with a small change in U_{air}, a feather would abruptly begin relatively large-amplitude, limit-cycle oscillations (Fig. 3) and concomitant sound production. Above U^*, we suggest that the relationship between the independent (aeroelastic deformation, orientation, size, shape, stiffness and U_{air}) and dependent variables (mode of flutter, loudness, amplitude and frequency) can vary, because the aeroelastic feedback between the aerodynamic and structural (inertial/elastic) forces experienced by the feather is sensitive to geometry (i.e. aeroelastic deformation, shape and orientation).

Because of constraints inherent to the SLDV system, our measurements of average vibration amplitude ($V_{feather}$) above U^* (within range III) were biased. Apparent declines in flutter amplitude with increases in U_{air} (e.g. red points in Fig. 3) may be solely attributable to this limitation. Nonetheless, based on observation of high-speed video of fluttering feathers, we suggest that the relationship between flutter amplitude and U_{air} does vary among the feathers sampled. Specifically, at U^* the feathers rapidly transitioned from essentially static (immobile) to a large amplitude, limit-cycle oscillation. Flutter amplitude intrinsically has a maximum (Bisplinghoff et al., 1996), and some feathers appeared to approach such a maxima almost immediately above U^*. As a result of this, further increases in U_{air} did not result in significant increases in amplitude. We suggest that this is the reason five feathers exhibited a negative correlation between U_{air} and sound loudness (Fig. 4A). This pattern was real, not merely experimental error.

By contrast, in the remaining feathers we measured, there appeared to be a strong correlation between U_{air} and flutter amplitude, with an amplitude maxima reached at a U_{air} well above U^*. We suggest that these are the feathers for which sound loudness increased with increasing U_{air} [see also fig. 1B in Clark et al. (Clark et al., 2011a)]. This assumes that flutter amplitude and sound loudness are tightly coupled, as fluctuations of both pressure and particle velocity of a packet of air at the surface of the feather will be proportional to the feather's displacement.

This variable scaling of loudness with U_{air} has an important implication for studies of the function of these sounds. Sound loudness may play a role in the function of a sound, such as in courtship displays. Flight speed is easily behaviorally modified (e.g. by diving). Our data show that in many but not all cases (Fig. 5A), maximizing speed will maximize sound loudness. Therefore, many birds have the option of modulating sound loudness by modulating speed. However, this is not true of all feathers, so for studies of sound function, this should be verified experimentally.

There are several possible sources of error in our measurements of loudness that make our measurements of SPL preliminary (Fig. 4). Only one microphone was used in our setup which, as a result of wind tunnel constraints, was downstream of the feather (Fig. 2B). The feathers can be imagined as dipole sound sources with maximum sound intensity radiated parallel to the axis of maximum vibration, which was perpendicular to flow (Blake, 1986; Manela and Howe, 2009b). If so, the downstream location of the microphone was in a relatively weak part of the sound field. We took care to avoid placing the microphone in the turbulent aerodynamic wake of the feathers, but for sounds below ~3 kHz the microphone was less than 1 wavelength from the feather, so near-field effects (such as local loudness maxima or minima) may be present. As the sound field shifted in shape slightly with each change in U_{air}, some changes in loudness may be attributable to near-field effects – although as the speed range tested was entirely Mach<0.1, this effect may have been negligible. In all, as sound loudness is clearly a salient feature of flutter-induced sounds that are incorporated into displays, multi-microphone experiments to quantify directionality of the sound field of a fluttering feather are warranted.

Airflow and orientation-induced changes in feather aeroelastic bending seemed to greatly influence the dynamics of sound production of some of the feathers. The white-bellied woodstar (*C. mulsant*) R4 was a singular example, in which changes in aeroelastic deformation caused continuous variation in the pitch of the sound produced, rather than discrete jumps from mode to mode as observed in other feathers [see fig. 2 in the companion paper (Clark et al., 2013)]. More subtle examples of the role of feather aeroelastic deformation were present in some of the feathers exhibiting tip modes (Clark et al., 2011a), particularly those of inner rectrices of *Selasphorus* sp. These feathers tended to express relatively few modes of flutter, and this seemed to be caused by changes in the feather's orientation that resulted in compensatory changes in aeroelastic bending, such that the tip of the feather had approximately the same geometry relative to airflow across a wide range of orientations and aeroelastic deformation. As a result, the feather tended to express the same mode of flutter, and mode of flutter was relatively insensitive to orientation. We hypothesize that if aeroelastic bending and mode of flutter could be controlled, all of the feathers would exhibit a positive correlation between U_{air} and frequency (Fig. 5). We suspect that the counter-examples (Clark et al., 2013) (Fig. 5) are the result of changes in feather aeroelastic deformation caused by changes in U_{air}. Likewise, for many of the feathers the relative strength of harmonics varied with changes in U_{air}, which may have been caused by small changes in aeroelastic deformation that slightly changed the mode shape of flutter.

There are several obvious avenues for future research. The setup we used was not ideal for varying orientation or quantifying aeroelastic bending. The data in this paper derive entirely from single feathers, because this is a comparatively simple experimental paradigm. Adding a second feather to the experiments presented here would introduced several additional degrees of freedom to the geometry. But feather–feather interactions are likely widespread, as birds typically have multiple adjacent feathers with modified shape, and we have demonstrated that feather–feather interactions do significantly modify the sounds produced by flutter (Clark, 2011; Clark et al., 2011a). Finally, in our experiments, both the air and

the feather were non-accelerating, whereas in a flying bird this will rarely be the case. Both acceleration reaction (caused by accelerating fluid) and a feather's inertial loading (caused by a feather's acceleration) could cause feathers to dynamically deform and adopt geometries not observed in static tests such as those done here. It remains unclear what role such transients may play in the dynamics of flutter and the sounds that are generated.

LIST OF SYMBOLS AND ABBREVIATIONS

f	frequency
L	length scale, relative to relevant mode of vibration or flow regime
R1–5	tail feathers (rectrices): R1, innermost; R5, outermost
SLDV	scanning laser Doppler vibrometer
SPL	sound pressure level
St	Strouhal number (fL/U_{air})
U_{air}	airspeed
U^*	critical airspeed at which aerodynamic energy exceeds damping, and the feather enters limit-cycle flutter
α	angle of attack: angle of the feather relative to airflow, corresponding to rotation about the Y-axis, parallel to the feather's calamus
β	sweep angle: angle of the feather relative to airflow, corresponding to rotation about the Z-axis, perpendicular to the plane of the feather vane

ACKNOWLEDGEMENTS

We are indebted to three anonymous reviewers for helpful comments, Glenn Weston-Murphy in the Mechanical Engineering Department at Yale University for support and access to the wind tunnel, and to Anand Varma for use of two photos.

AUTHOR CONTRIBUTIONS

C.J.C. and R.O.P. initiated the study; C.J.C. collected and analyzed wind tunnel data while D.O.E. provided SLDV; R.O.P. provided equipment and support; all authors contributed to writing the paper.

COMPETING INTERESTS

No competing interests declared.

FUNDING

This work was supported by the National Science Foundation [grant no. IOS-0920353 to R.O.P. and C.J.C.].

REFERENCES

Alben, S. and Shelley, M. J. (2008). Flapping states of a flag in an inviscid fluid: bistability and the transition to chaos. *Phys. Rev. Lett.* **100**, 074301.
Argentina, M. and Mahadevan, L. (2005). Fluid-flow-induced flutter of a flag. *Proc. Natl. Acad. Sci. USA* **102**, 1829-1834.
Bahr, P. H. (1907). On the 'bleating' or 'drumming' of the snipe (*Gallinago coelestis*). In *Proceedings of the Zoological Society of London,* Part 1, pp. 12-35.
Bahr, P. H. and Pye, J. D. (1985). Mechanical sounds. In *A Dictionary of Birds* (ed. B. Campbell and E. Lack). Vermillion, SD: Buteo Books.
Bearman, P. W. (1984). Vortex shedding from oscillating bluff bodies. *Annu. Rev. Fluid Mech.* **16**, 195-222.
Bisplinghoff, R. L., Ashley, H. and Halfman, R. L. (1996). *Aeroelasticity*. Mineola, NY: Dover Publications, Inc.
Blake, W. K. (1986). *Mechanics of Flow-Induced Sound And Vibration*. Orlando, FL: Academic Press, Inc.
Bonser, R. H. and Purslow, P. P. (1995). The Young's modulus of feather keratin. *J. Exp. Biol.* **198**, 1029-1033.
Bostwick, K. S. and Prum, R. O. (2003). High-speed video analysis of wing-snapping in two manakin clades (Pipridae: Aves). *J. Exp. Biol.* **206**, 3693-3706.
Bostwick, K. S. and Prum, R. O. (2005). Courting bird sings with stridulating wing feathers. *Science* **309**, 736.
Brush, A. H. (1983). Self-assembly of avian ϕ-keratins. *J. Protein Chem.* **2**, 63-75.
Carr-Lewty, R. A. (1943). The aerodynamics of the drumming of the common snipe. *Br. Birds* **36**, 230-234.
Chanaud, R. C. (1970). Aerodynamic whistles. *Sci. Am.* **223**, 40-46.
Clark, C. J. (2008). Fluttering wing feathers produce the flight sounds of male streamertail hummingbirds. *Biol. Lett.* **4**, 341-344.
Clark, C. J. (2011). Wing, tail, and vocal contributions to the complex signals of a courting Calliope hummingbird. *Curr. Zool.* **57**, 187-196.
Clark, C. J. and Feo, T. J. (2008). The Anna's hummingbird chirps with its tail: a new mechanism of sonation in birds. *Proc. Biol. Sci.* **275**, 955-962.
Clark, C. J. and Feo, T. J. (2010). Why do Calypte hummingbirds 'sing' with both their tail and their syrinx? An apparent example of sexual sensory bias. *Am. Nat.* **175**, 27-37.
Clark, C. J., Elias, D. O. and Prum, R. O. (2011a). Aeroelastic flutter produces hummingbird feather songs. *Science* **333**, 1430-1433.
Clark, C. J., Feo, T. J. and Escalante, I. (2011b). Courtship displays and natural history of the scintillant (*Selasphorus scintilla*) and volcano (*S. flammula*) hummingbirds. *Wilson J. Ornithol.* **123**, 218-228.
Clark, C. J., Elias, D. O., Girard, M. B. and Prum, R. O. (2013). Structural resonance and mode of flutter of hummingbird tail feathers. *J. Exp. Biol.* **216**, 3404-3413.
Darwin, C. (1871). *The Descent of Man, and Selection in Relation to Sex*. Princeton, NJ: Princeton University Press.
Fletcher, N. H. (1992). *Acoustic Systems in Biology*. New York, NY: Oxford University Press.
Fletcher, N. H. and Rossing, T. D. (1998). *The Physics of Musical Instruments*. New York, NY: Springer-Verlag.
Howe, M. S. (2008). *Acoustics of Fluid-Structure Interactions*. Cambridge: Cambridge University Press.
Hunter, T. A. (2008). On the role of wing sounds in hummingbird communication. *Auk* **125**, 532-541.
Lentink, D., Van Heijst, G. F., Muijres, F. T. and Van Leeuwen, J. L. (2010). Vortex interactions with flapping wings and fins can be unpredictable. *Biol. Lett.* **6**, 394-397.
Lighthill, M. J. (1952). On sounds generated aerodynamically. I. General theory. *Proc. R. Soc. A* **211**, 564-587.
Mandre, S. and Mahadevan, L. (2010). A generalized theory of viscous and inviscid flutter. In *Proceedings of the Royal Society Mathematical, Physical and Engineering Sciences Series A* **466**, 141-156.
Manela, A. and Howe, M. S. (2009a). The forced motion of a flag. *J. Fluid Mech.* **635**, 439-454.
Manela, A. and Howe, M. S. (2009b). On the stability and sound of an unforced flag. *J. Sound Vib.* **321**, 994-1006.
McGuire, J. A., Witt, C. C., Remsen, J. V., Dudley, R. and Altshuler, D. L. (2009). A higher-level taxonomy for hummingbirds. *J. Ornithol.* **150**, 155-165.
Miller, S. J. and Inouye, D. W. (1983). Roles of the wing whistle in the territorial behavior of male broad-tailed hummingbirds (*Selasphorus platycercus*). *Anim. Behav.* **31**, 689-700.
Nash, E. C., Lowson, M. V. and McAlpine, A. (1999). Boundary-layer instability noise on aerofoils. *J. Fluid Mech.* **382**, 27-61.
Prum, R. O. (1998). Sexual selection and the evolution of mechanical sound production in manakins (Aves: Pipridae). *Anim. Behav.* **55**, 977-994.
Rayleigh, Lord (1915). Æolian tones. *Philos. Mag.* **29**, 433-444.
Reddig, E. (1978). Der ausdrucksflug der bekassine (*Capella gallinago gallinago*). *J. Ornithol.* **119**, 357-387.
Schnipper, T., Andersen, A. and Bohr, T. (2009). Vortex wakes of a flapping foil. *J. Fluid Mech.* **633**, 411-423.
Soderman, P. T. and Allen, C. S. (2002). Microphone measurements in and out of airstream. In *Aeroacoustic Measurements* (ed. T. J. Mueller). New York, NY: Springer.
van Casteren, A., Codd, J. R., Gardiner, J. D., McGhie, H. and Ennos, A. R. (2010). Sonation in the male common snipe (*Capella gallinago gallinago* L.) is achieved by a flag-like fluttering of their tail feathers and consequent vortex shedding. *J. Exp. Biol.* **213**, 1602-1608.
Williamson, C. H. K. and Gorvardhan, R. (2004). Vortex-induced vibrations. *Annu. Rev. Fluid Mech.* **36**, 413-455.
Zhang, J., Childress, S., Libchaber, A. and Shelley, M. (2000). Flexible filaments in a flowing soap film as a model for one-dimensional flags in a two-dimensional wind. *Nature* **408**, 835-839.

Supplemental Figures and Tables.

Table S1. Feathers tested in this study, sample size in parentheses. Width (chord) measured at ¾ of the length of the feather, i.e. before tapering. See also Fig. 5 for drawings of feather shape.

Species	Feather (N)	Width, *w* (mm)	Length *l* (mm)	Feather Mass (mg)	Estimated Added Mass (mg)[1]
Anna's Hummingbird *Calypte anna* Lesson 1829	R5 (2)	3.5	32	4.4	0.37
Costa's Hummingbird *Calypte costae* Bourcier 1839	R5 (1)	1.6	22	0.8	0.054
Costa's Hummingbird	R4 (1)	3.9	23	1.4	0.34
Black-chinned Hummingbird *Archilochus alexandri* Bourcier and Mulsant 1846	R5 (2)	3.8	23	1.5	0.32
Black-chinned Hummingbird	R4 (1)	5.2	25	1.6	0.65
Ruby-throated Hummingbird *Archilochus colubris* Linnaeus 1758	R5 (1)	3.5	25	1.2	0.29
Allen's Hummingbird *Selasphorus sasin* Lesson 1829	R5 (1)	1.4	19	0.7	0.036
Allen's Hummingbird	R4 (2)	1.9	19	0.8	0.066
Allen's Hummingbird	R3 (1)	3.4	22	0.9	0.24
Allen's Hummingbird	R2 (1)	3.6	22	1.3	0.27
Rufous Hummingbird *S. rufus* Gmelin 1788	R5 (1)	2.6	20	0.9	0.13
Rufous Hummingbird	R4 (1)	3.6	24	1.0	0.30
Rufous Hummingbird	R3 (1)	4.7	*24*	1.3	0.51
Rufous Hummingbird	R2 (1)	6.0	26	1.3	0.90
Broad-tailed Hummingbird *S. platycercus* Swainson 1827	R2 (1)	6.7	32	2.0	1.4
Scintillant Hummingbird *S. scintilla* Gould 1850	R2 (1)	5.8	25	1.1	0.80
Volcano Hummingbird *S. flammula torridus* Salvin 1870	R2 (1)	6.9	26	1.3	1.2
Volcano Hummingbird	R3 (1)	6.5	27	1.6	1.1
Calliope Hummingbird *S. calliope* Gould 1847	R3 (1)	5.4	19	1.5	0.53
Calliope Hummingbird *S. calliope*	R2 (1)	5.2	18	1.3	0.47
Calliope Hummingbird *S. calliope*	R1 (1)	4.6	16	1.2	0.32
White-bellied Woodstar *Chaetocercus mulsant* Bourcier 1842	R4 (2)	0.88	24	1.7	0.018
White-bellied Woodstar	R3 (1)	3.2	25	0.7	0.25
Magenta-throated Woodstar	R5 (1)	3.5	34	2.5	0.40

Philodice bryantae Lawrence 1867					
Purple-throated Woodstar *P. mitchellii* Mulsant and Verreaux 1866	R5 (1)	2.4	30	1.8	0.17
Purple-throated Woodstar	R4 (1)	3.5	32	1.7	0.38
Bahama Sheartail *Calothorax e. evelynae* Bourcier 1847	R5 (1)	4.4	30	2.2	0.56

[1] estimated as a cylinder of air around the feather, = $\rho w^2 l\pi/4$.

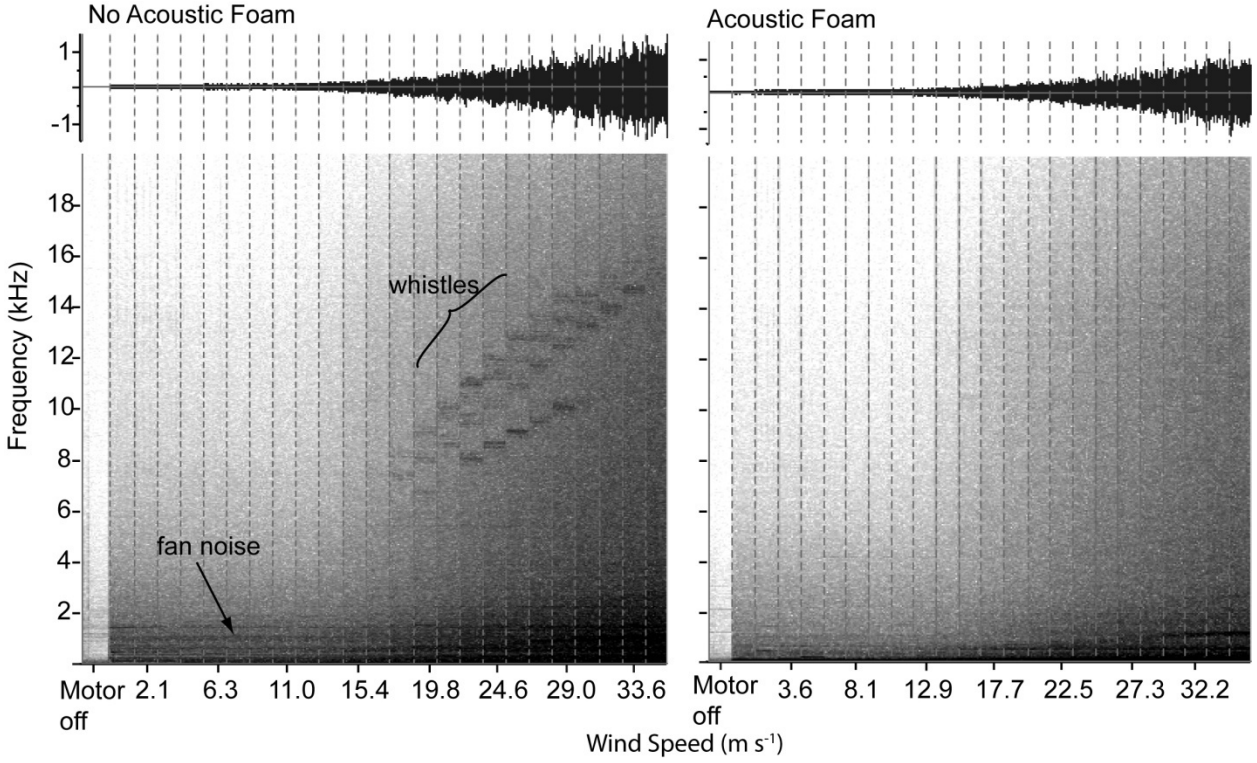

Figure S1. Waveform (above) and sound spectrograms (below) of the background sound of the wind tunnel as a function of airspeed (U_{air}), without (left) and with (right) acoustic treatment of the wind tunnel. Sound samples separated by dashed lines. Each sample is of 5 seconds of sound, recorded at a fixed U_{air}. Without the acoustic foam, interval between samples is 1.48 m s^{-1}; with the foam, interval is 1.58 m s^{-1}. The motor of the wind tunnel produced significant levels of sound, even with the fan off (compare 'motor off' sample to its neighbor); at higher U_{air}, fixtures within the tunnel created aerodynamic whistles that were individually eliminated.

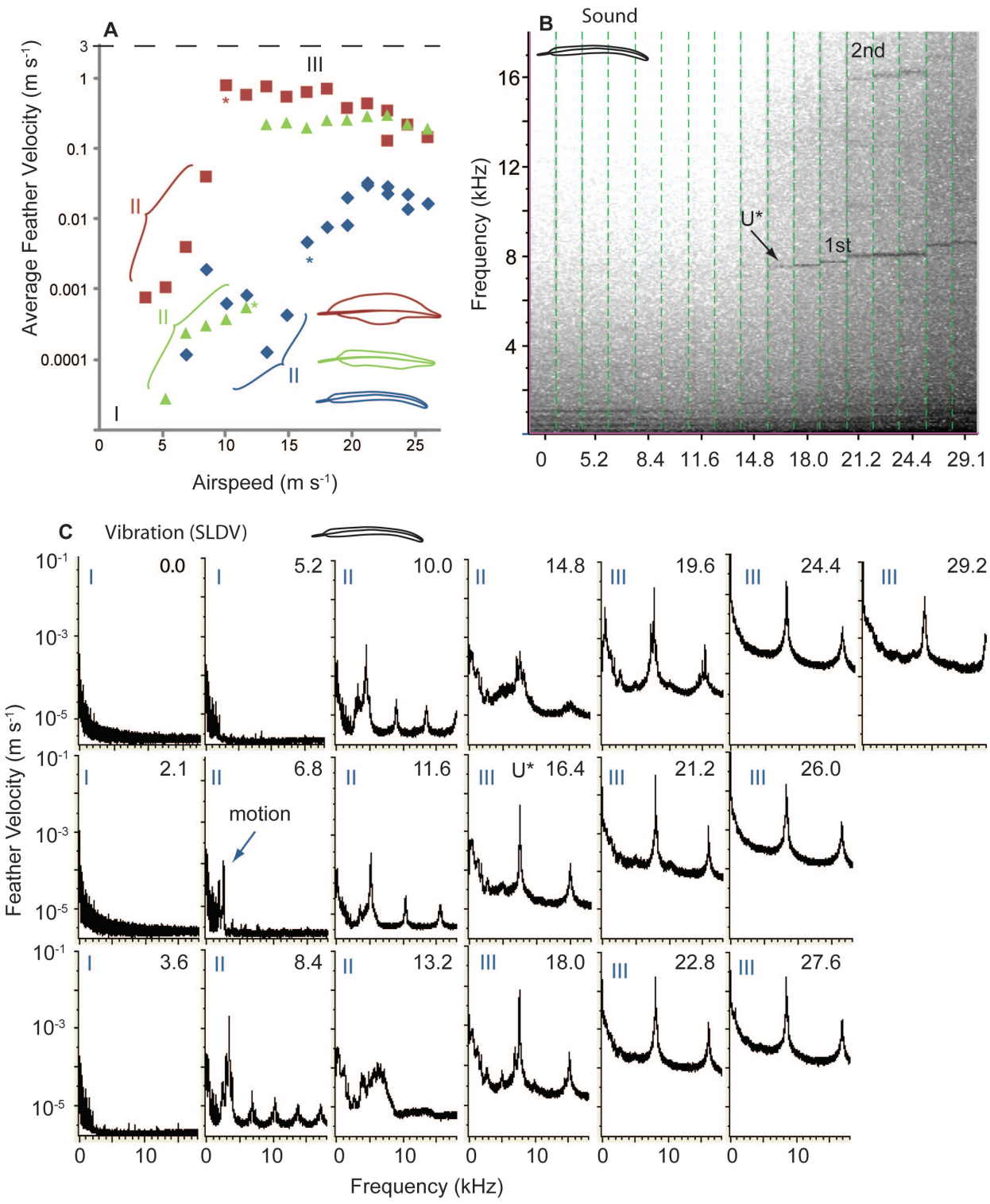
A
Average Feather Velocity (m s-1)
Airspeed (m s-1)
I
II
III
B
Sound
2nd
1st
U*
Frequency (kHz)
C
Vibration (SLDV)
motion
Feather Velocity (m s-1)
Frequency (kHz)

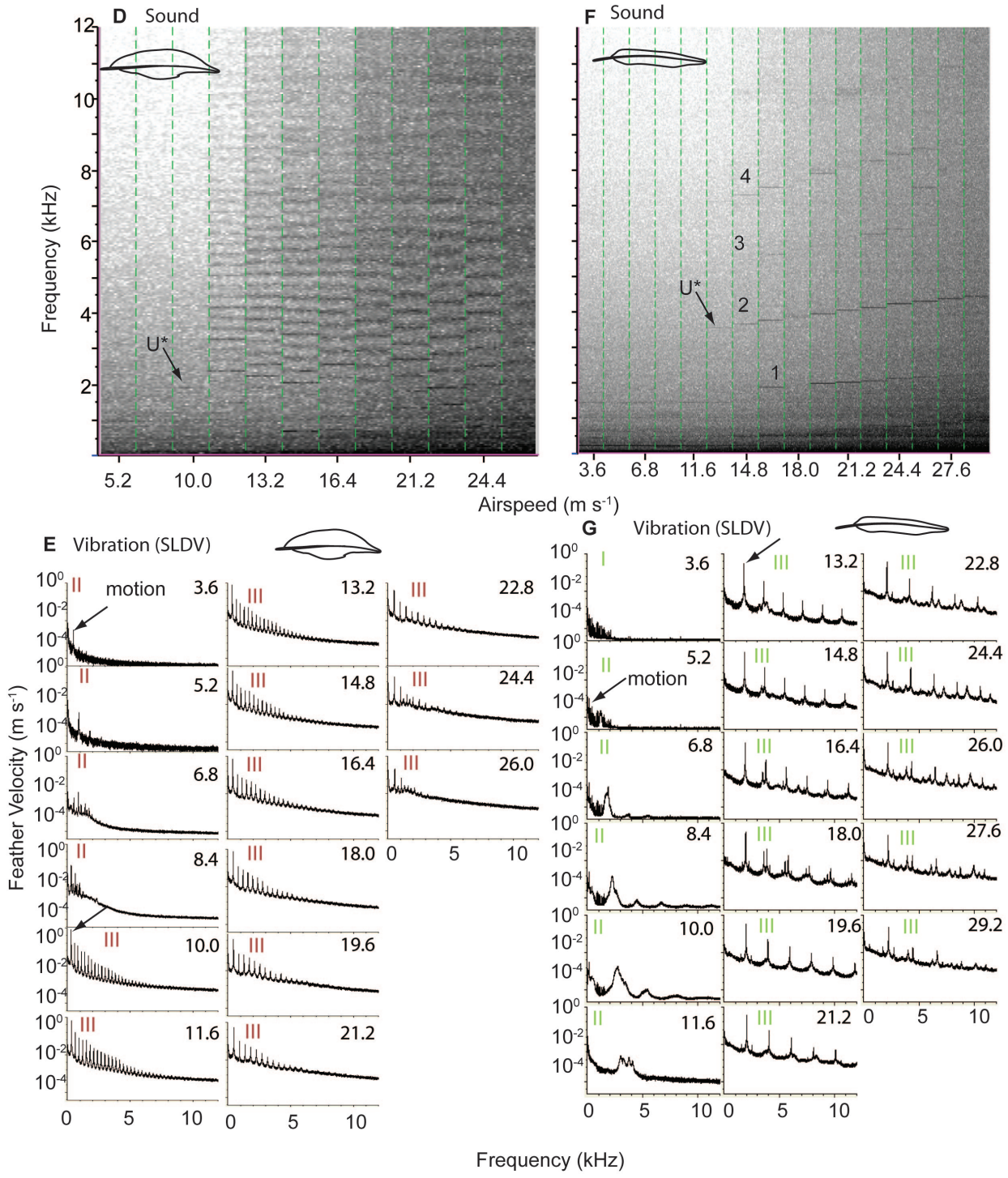

Figure S2. Sound production and flutter amplitude as a function of airspeed (U_{air}), for the hummingbird tail-feathers Costa's R5 (blue), Broad-tailed R2 (red), and Black-chinned R5 (green). **A**. Velocity of the peak frequency of vibration as a function of airspeed. All feathers exhibited varying magnitudes of flutter that fit into three ranges. Range I: at low U_{air}, no motion

was detected (no data present). Range II: at intermediate U_{air}, small amplitude vibrations recorded, but no sound detected (brackets). * = sound was first detected. The transition from range II to range III occurs at a critical velocity (U^*) characterized by an abrupt increase in vibration velocity. The SLDV had a maximum velocity of 3 m s^{-1} (dashed line) that biases downward the points in range III. **B**-**G**. sound spectrograms from Costa's R5 (**B**), Broad-tailed R2 (**D**), and Black-chinned R5 (**F**) over a range of U_{air}, accompanied by the corresponding velocity spectra for the fluttering feather (**C**, **E**, **G**). In **B**, **D**, and **F**, spectrograms from a 5-second sample of sound are each separated by a green dashed line. The speed at which sound was first detected is indicated with an asterisk; f, fundamental frequency; numbers are harmonics. In **F**, the fundamental frequency is difficult to see against the background sound of the tunnel. Feather velocity measured by SLDV is the average value of up to ~100 points across the feather.